REVIEW

Organic Stereochemistry

Part 6[1])

The Conformation Factor in Molecular Pharmacology

by **Giulio Vistoli**[a]), **Bernard Testa***[b]), and **Alessandro Pedretti**[a])

[a]) Dipartimento di Scienze Farmaceutiche, Università degli Studi di Milano, Via Mangiagalli, 25, I-20133 Milano

[b]) Department of Pharmacy, Lausanne University Hospital (CHUV), Rue du Bugnon, CH-1011 Lausanne (e-mail: Bernard.Testa@chuv.ch)

Following the previous *Part* on the mechanisms of chiral recognition in pharmacology, the road was open to cover one aspect of stereoselectivity that had been evoked in *Part 5* but not discussed explicitly, namely the pharmacological significance of the conformational behavior of active molecules. There, we saw how ligands and binding sites adapt to each other, but these results were not related explicitly to the conformational behavior of the ligand. The focus of the present *Part* is to use a few well-known drugs, examine their conformational behavior, compare the 3D geometry of probable conformers with rigid analogs acting at the same receptor, and reflect on the concept of 'active conformation'.

This *Part 6* continues our series of reviews on stereochemistry, its guiding principles, and biomedicinal relevance. Following a detailed exposition of configurational isomerism in *Parts 1–3*, *Part 4* introduced readers to *conformational isomerism*, its nomenclature, and its occurrence in linear and cyclic systems. Thus, the four *Parts* covered the large field of structural stereochemistry and its principles. Thereafter, our focus changed to the exploration of *the biomedicinal relevance of stereochemistry. Part 5* dealt specifically with the mechanisms of chirality recognition (commonly known as chiral recognition) in pharmacology and provided ample illustration of enantio- and diastereoselectivity in molecular and clinical pharmacology.

Following *Part 5*, the road is now open to cover an important aspect of stereoselectivity that was mentioned in *Part 5* but not discussed explicitly, namely the pharmacological significance of the conformational behavior of bioactive molecules. Specifically, *Part 5* hinted at the role of conformational factors in drug–receptor recognition using unpublished molecular-modeling work showing, in great graphical detail, the docking of (*S*)-hyoscyamine to human muscarinic receptors. There, we saw how ligands and binding sites adapt to each other, but these results were not placed in the broader context of a ligand's conformational behavior.

---

[1]) For the other *Parts*, see *Helv. Chim. Acta* **2013**, *96*, 1–3.

The focus of the present *Part* is thus to use a few well-known drugs and explore their conformational space by using simple computational tools. In some cases, the 3D geometry of probable conformers is compared with that of rigid analogs acting at the same receptor, with a view to gaining some insight into '*bioactive conformations*'. However, it must be stressed from the outset that this approach is merely didactic and is in no way intended to provide novel results on which drug design could be based. The influence of solvation coupled with docking simulations is explored using muscarinic agents. The *Part* concludes with a complex case of nomenclature.

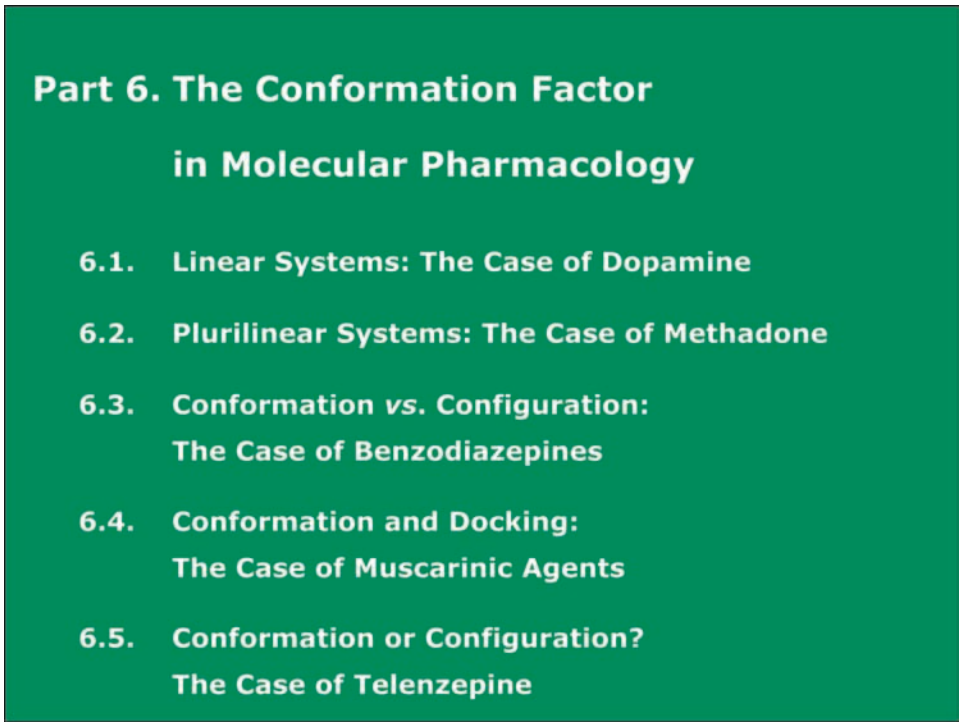

Fig. 6.1. *Part 6* focuses of the conformational behavior of a few selected drugs acting on important pharmacological receptors. The aim in the first two examples is to compare the results of our conformational searches with the 3D geometry of rigid analogs acting on the same receptors. By doing so, insights can be obtained on the 'active conformation' of a given flexible drug, taking into account the energy penalty needed to reach such conformations. The search for active conformations has been and remains a productive field of investigation [1–14]. *Dopamine* was chosen as a relatively straightforward example, given that its 3D geometry depends essentially on two degrees of conformational freedom in its linear side chain. With its two functionalized chains, *methadone* offers a structurally more complex example of conformation-dependent activity.

Our third example, *diazepam*, has a flexible seven-membered ring which accounts for the occurrence of two enantiomeric conformers differing in their biological significance, as verified with 3-substituted chiral analogs. The fourth example searches for the active conformation of *muscarinic agents*, by using receptor docking simulations which complement the study on hyoscyamine and muscarinic receptors presented in *Part 5*. *Part 6* concludes with *telenzepine*, comparing the conformational behavior of its side chain and the high configurational stability of its ring system, and the nomenclature issue it raises.

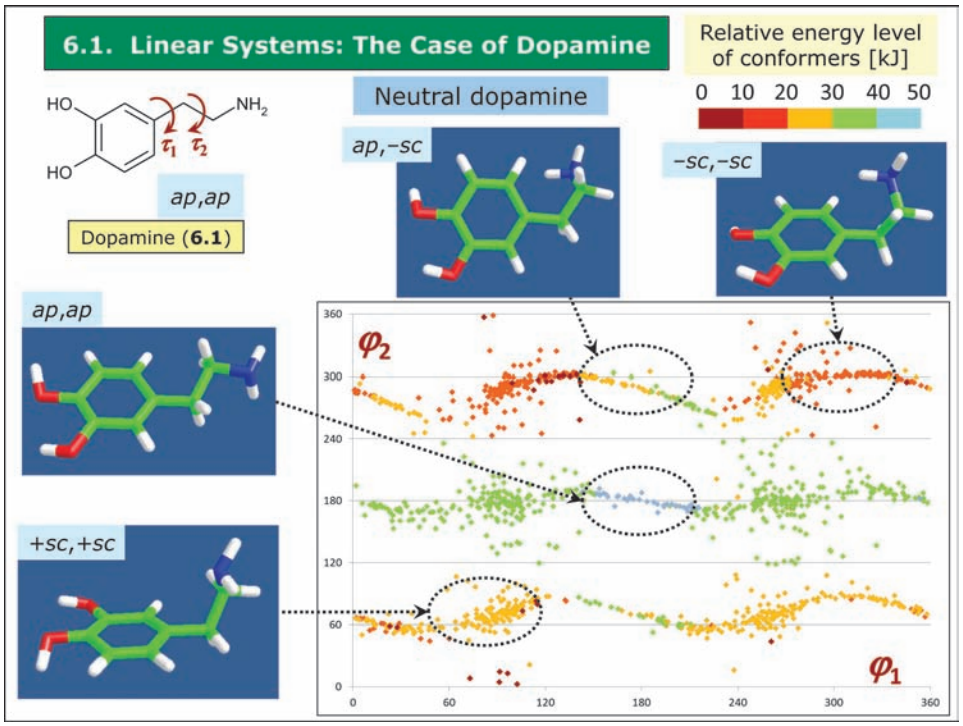

Fig. 6.2. Our first illustration of the conformational space of a medicinally relevant compound is that of the neurotransmitter *dopamine* (**6.1**), the endogenous ligand of the dopaminergic receptors. Besides its prominent biological role, dopamine was selected for *its structural simplicity*, since its pharmacologically relevant conformational profile is completely defined by *two rotatable bonds* (neglecting rotation of the two OH groups and the NH_2 group). The torsion angles τ_1 and τ_2 describe the conformation around these two bonds. Specifically, the angle τ_1 describes the orientation of the phenyl ring relative to the ethyl chain, while the angle τ_2 refers to the geometry of the alkyl chain and as such plays a major role as a descriptor of the distance between the NH_2 group and the aromatic ring [1][15].

Given its number of rotors, the conformational space of *neutral dopamine* can be explored by an *in vacuo*-quenched systematic search in which the two rotors are systematically rotated[2]). The resulting plot (in the φ_1 and φ_2 scale) reports the conformers generated by the search and colored according to their potential energy, showing that both dihedral angles can assume *synclinal* (τ *ca.* 60° and *ca.* 300°) and *antiperiplanar* geometries (τ *ca.* 180°). This yields *nine possible conformational clusters*, even though the folded conformations characterized by *synclinal* geometries are clearly

[2]) The conformational profiles of neutral and protonated dopamine was investigated by systematically rotating the two rotatable bonds by 10° steps, thus generating 1296 (36×36) conformers. After a preliminary minimization to discard high-energy geometries, the potential energy of the optimized conformations was computed by a PM6 semi-empirical method. For further details, see the *Footnote* to *Fig. 5.10* in *Part 5*.

favored, while the more extended conformations in which τ_1 and/or τ_2 assume an *antiperiplanar* geometry can roughly be seen as transition forms connecting the four folded and preferred conformations. The preference for folded conformations is in line with several reported studies and is clearly ascribable to the stabilizing intramolecular weak H-bonds between the NH_2 group and the phenyl ring. Interestingly, the four folded conformers are not completely equivalent. Depending on the value of τ_1, the N-atom is proximal to the *meta*-OH group in two clusters and distal in the two other cases. The plot even reveals that the distal conformers of neutral dopamine are slightly more stable than the proximal ones, presumably due to a weak repulsion between electron-rich atoms.

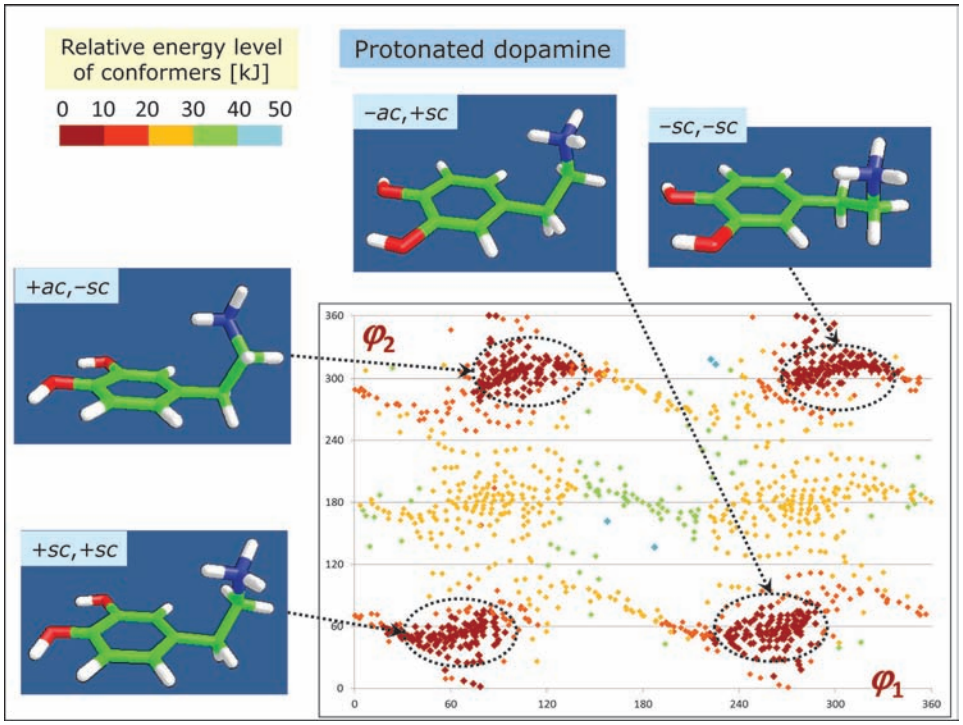

Fig. 6.3. This *Figure* illustrates the conformational profile of *protonated dopamine* and shows a τ_1 *vs.* τ_2 plot (in the φ_1 and φ_2 scale) comparable to that found for neutral dopamine in which the four folded conformations appear to be clearly more stable than those characterized by *antiperiplanar* geometries. Specifically, the conformational space of protonated dopamine seems to be heavily influenced by a stabilizing intramolecular π–cation interaction between the ammonium head and the phenyl ring. Such a *charge-transfer interaction* removes part of the difference between folded conformations which become more similarly favored regardless of the distance between the ammonium head and the *meta*-OH group. Overall, a comparison of *Figs. 6.2* and *6.3* emphasizes that the conformational profile of dopamine is quantitatively more than qualitatively affected by the ionization state, with *synclinal* geometries being favored irrespective of the simulated pH value.

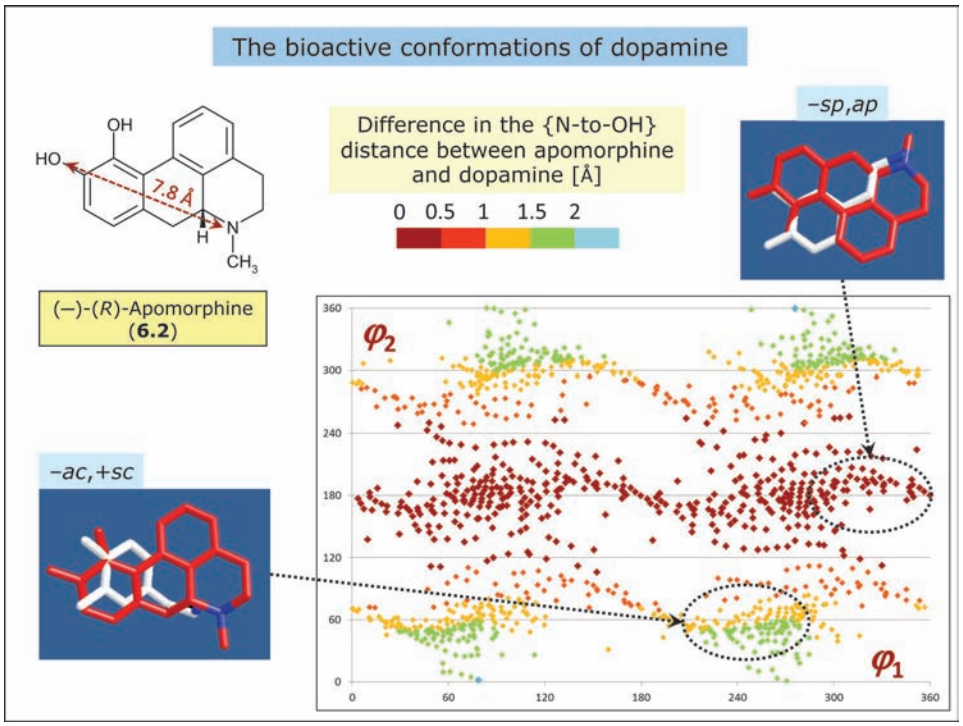

Fig. 6.4. As seen in the previous *Figures* and discussed in *Part 4*, the *conformational profile* of a given molecule can be explored exhaustively by calculating the energy profile of a set of representative geometries. In contrast, *identifying the bioactive conformation* of a molecule, namely a conformation which optimizes its interaction with the biological target, cannot be confidently deduced from the energy profile but requires different approaches. When the 3D structure of the biomacromolecular target is available, one or more bioactive conformation(s) may be revealed by docking simulations (see below *Figs. 6.11*, *6.13*, and *6.14*). Should this prove unfeasible, one can approach the problem by comparing the probable conformations of a ligand with the structure of an *active and rigid analog* which, by definition, can assume only one conformation.

The identification of the putative bioactive conformer(s) of dopamine can be attempted by comparing it with *(*R*)-apomorphine* (**6.2**), a rigid dopaminergic agonist. Specifically, matching the single bioactive apomorphine conformation with energetically plausible dopamine conformations can be guided by comparing the fixed value of the key distance between the N-atom and the farther O-atom for apomorphine ($d =$ 7.8 Å) with the values for the corresponding distance in dopamine (ranging from 5.8 Å for folded geometries to 8.0 Å for extended conformations). On these grounds, *Fig. 6.4* shows a τ_1 *vs.* τ_2 plot (in the φ_1 and φ_2 scale) of dopamine colored by the difference in the N-to-OH distance between apomorphine and dopamine. It is evident that such a plot is almost the opposite of the plot of conformational energy depicted in *Fig. 6.3*. Indeed, the putative bioactive conformers of dopamine, namely those whose

distance most resembles that in apomorphine, are the energetically less favored, extended ones, whereas, in the energetically favored folded geometries, the N- and O-atoms are too close to each other to mimic apomorphine. The plot presented here also shows that several conformational clusters of dopamine meet the distance criterion (*i.e.*, $+sc,ap$; $+ac,ap$; $-ac,ap$; $-sc,ap$), suggesting that several putative bioactive conformations can occur whose key groups have a suitable arrangement to optimize receptor binding.

This example shows that there is no stringent relation between bioactive and lowest-energy conformations. This is understandable, since the energy differences between the conformers of dopamine monitored here are small enough to be counterbalanced by the energy gained from the binding process. When such conditions are met, the bioactive conformation(s) may thus be different from the lowest-energy geometries; indeed, excessive energy differences would undermine affinity.

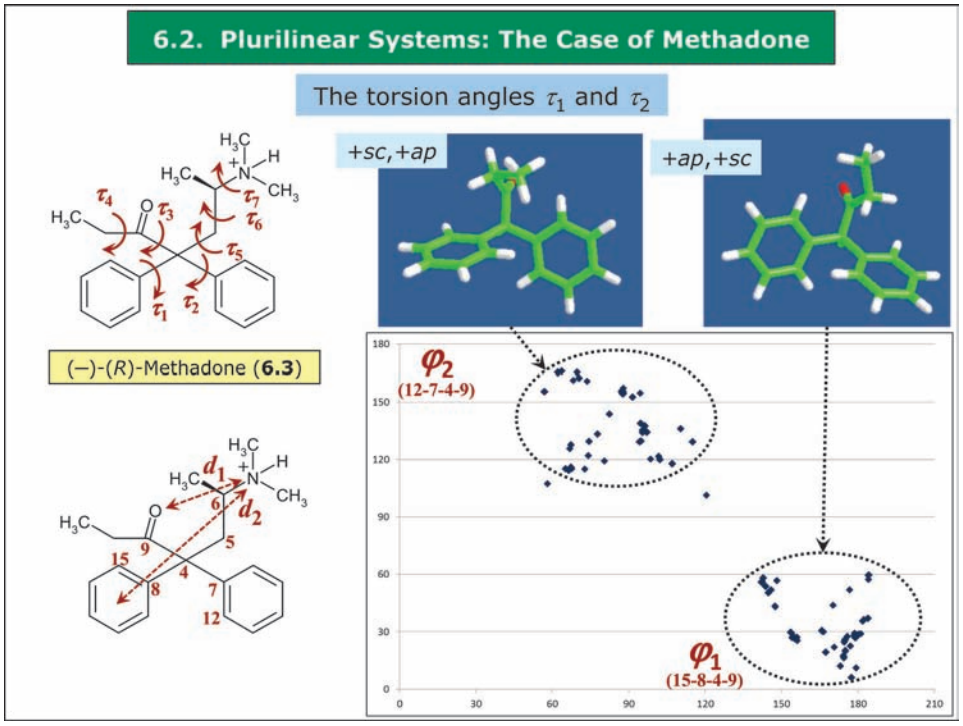

Fig. 6.5. The synthetic opioid *methadone* (**6.3**; arbitrary numbering of atoms and torsion angles) is an analgesic and anti-addictive drug used as the racemate, even though its (*R*)-enantiomer accounts for much of its activity [1]. The chemical structure of methadone is markedly more complex than that of dopamine, offering a greater challenge to identify active conformation(s) [16–19]. As represented in *Fig. 6.5*, the

conformational behavior of methadone was investigated in its protonated form, since this is the one known to be involved in receptor recognition[3]).

Seven rotatable bonds serve to characterize the conformational space of methadone, giving rise to numerous energetically plausible conformations. In an attempt to simplify the analysis, methadone was subdivided into fragments whose conformation can be examined separately; only two pairs of rotatable bonds were considered in turn. The first fragment comprises the Ph_2C moiety whose conformation is defined by two equivalent torsion angles (τ_1 and τ_2). As depicted in the corresponding φ_1 *vs.* φ_2 plot and irrespective of the conformational behavior of the remainder of the molecule, it appears that two possible arrangements of the Ph rings can minimize their mutual steric repulsion while maximizing intramolecular π–π stacking. These two arrangements are approximately mirror images and are defined as $+ap, +sc$ and $+sc, +ap$, respectively. Since these arrangements are in equilibrium and have minimal influence on the rest of the molecule, the conformation of the two side chains can be examined regardless of the arrangement assumed by the Ph rings.

The fragment comprising the 1-oxopropyl moiety includes the rotatable bonds defined by τ_3 and τ_4. The conformation of the former bond determines the arrangement of the C=O group; its flexibility is restricted, since τ_3 assumes almost exclusively *antiperplanar* conformations due to constraints imposed by the C_{sp^2}-atom and the Ph rings. The second rotatable bond shows a greater flexibility assuming both *synclinal* and *antiperiplanar* geometries, but since this merely determines the orientation of the distal Me group, it only marginally influences the conformational behavior of methadone.

---

[3]) The conformational profiles of protonated methadone was investigated by a quenched Monte Carlo simulation which produced 1,000 minimized conformations, whose potential energy was then computed by a PM6 semi-empirical method. For further details, see the *Footnote* to *Fig. 5.10* in *Part 5*.

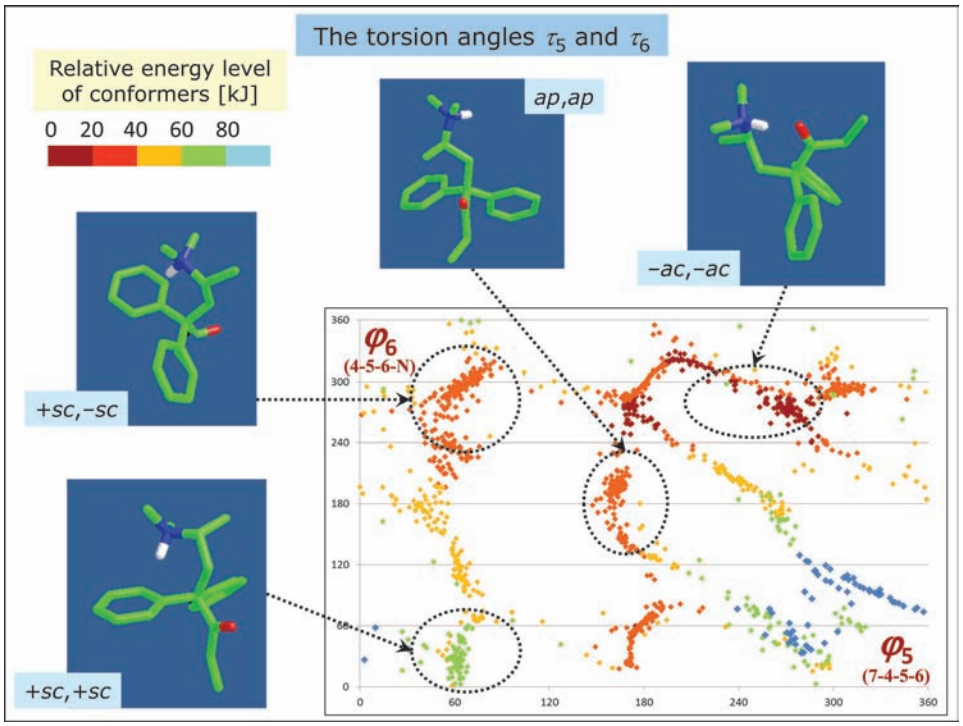

Fig. 6.6. The *alkylamine side chain* is the one which most strongly influences the conformational behavior and receptor recognition of methadone (**6.3**). The *critical bonds* in this side chain are described by their torsion angles τ_5 and τ_6. The corresponding φ_5 *vs.* φ_6 plot shows that both bonds can assume *synclinal* and *antiperiplanar* geometries, yielding nine possible conformational clusters. The resulting energy profile is complex and can best be understood by considering *three factors: a*) *steric hindrance* that favors extended conformations, a pharmacologically highly relevant outcome; *b*) the presence of a *reinforced intramolecular H-bond between the carbonyl O-atom and the ammonium head*, which counterbalances the energy cost of adopting folded geometries; and *c*) the fact that intramolecular π–cation interactions can only partially counter the steric hindrance of *synclinal* geometries. On these grounds, one notes that the most stable conformations are those stabilized by the H-bond mentioned above, even though this is far from ideal as confirmed by experimental and computational studies [16–19]. Interestingly, this H-bond forms a *seven-membered azepine pseudo-ring*, the presence of a N-containing heterocycle in synthetic opioids being a common feature [1][16]. In contrast, folded geometries stabilized by intramolecular charge-transfer interactions have energy levels sometimes comparable to those of extended conformations, but often markedly higher as seen for highly hindered conformers as in the case of the $+sc,+sc$ cluster.

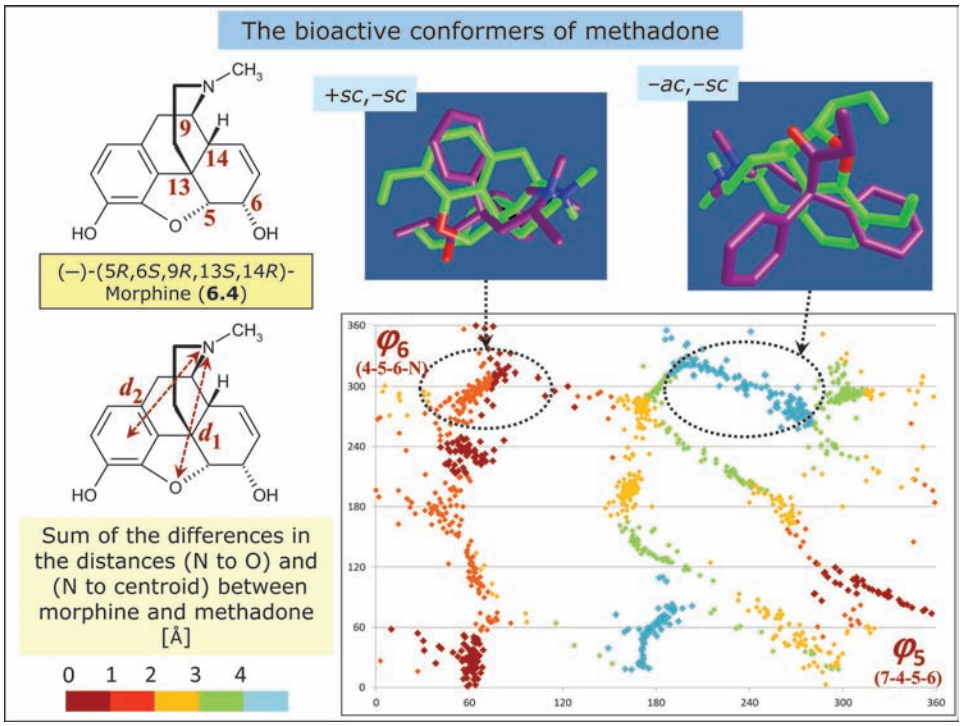

Fig. 6.7. The identification of the putative bioactive conformation(s) of methadone (**6.3**) is approached here by comparing it with *natural morphine* (**6.4**), the prototypal opioid agonist. When considering the structural complexity of both molecules, as well as the various moieties presumably involved in receptor recognition, steric matching cannot be guided by only one intramolecular distance (as could be done for dopamine *vs.* apomorphine) but must involve more than one geometrical descriptor. Specifically, two corresponding distances were compared here, namely *a*) d_1, the N^+–O distance (5.30 Å in morphine), and *b*) d_2, the distance between the ammonium head and the center of mass of the phenyl ring in morphine (5.53 Å) or the center of mass of the distal phenyl ring of methadone.

The φ_5 *vs.* φ_6 plot is colored by the *sum of the differences in the monitored distances* in morphine and in the computed methadone conformers. Clearly, all molecular geometries having τ_5 in the $+sc$ range indicate a good overlap between the two molecules, with the best overlap based on the two monitored distances being found among folded methadone geometries which bring its ammonium head and carbonyl O-atom in comparatively closer proximity (τ_6 being in the ranges $+sp$, $+sc$, $-ac$, and $-sc$). When considering the energy profile in the previous *Figure*, the best combination is afforded by the $+sc,-sc$ conformers which are of relatively low energy and show a satisfactory overlap between all matched pharmacophoric elements.

It is frequently observed that, despite steric factors, lower-energy geometries are normally stabilized *in vacuo* by *polar intramolecular interactions*, while, *in water*, *intermolecular interactions* between solvent and polar groups will tend to favor more

extended geometries. The same can be true in receptor interactions, where the polar groups in a ligand must be accessible and prone to recognition. This means that, in water or when interacting with a receptor, hydration or binding must account for the conformational costs required to overcome a possible preference for folded conformers and expose the interacting groups.

For simplicity's sake, we assumed that all opioid receptors (and earlier all dopaminergic receptors) have *identical structural requirements* and recognize the same bioactive conformations. This, however, is very far from being true since each binding site has its own features and prefers well-defined bioactive conformations. This implies that flexible molecules like methadone or dopamine can fine-tune their conformation and adapt themselves to optimize their recognition by different receptor subtypes, while more rigid ligands like morphine or apomorphine can meet the structural requirements of a restricted number of receptor subtypes, suggesting that selectivity and flexibility are, as a trend, contrasting factors.

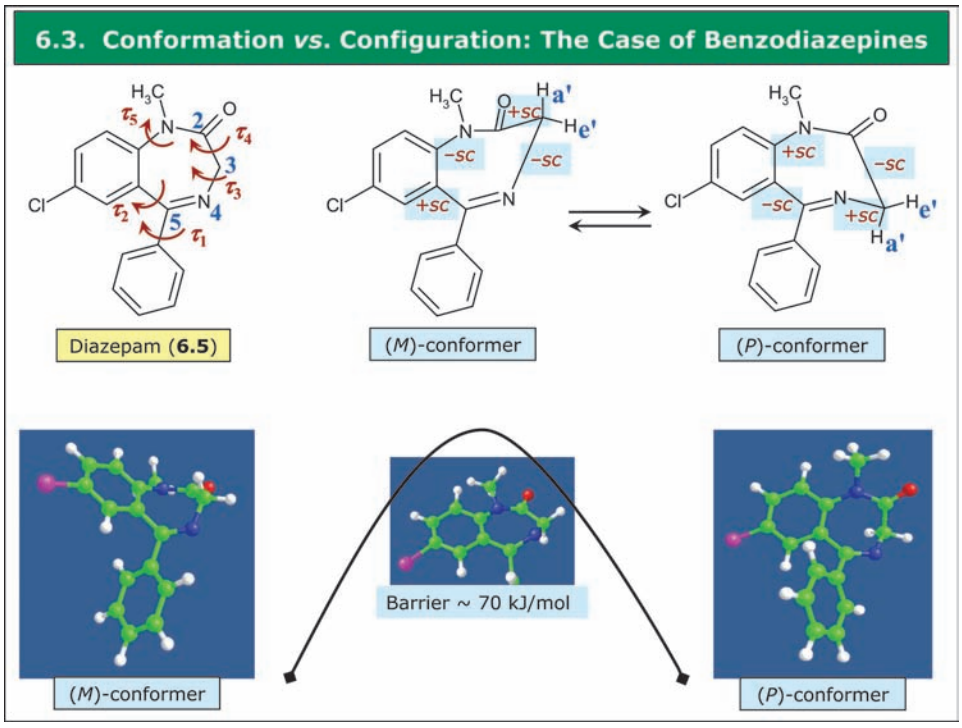

Fig. 6.8. As seen in *Part 4* when describing *ring systems and ring puckering*, cyclic molecules and moieties can also enjoy some degree of conformational flexibility which in turn may be biologically relevant.

A remarkable example of the key role of conformational transitions in cyclic compounds is afforded by the *1,4-benzodiazepines*, a well-known class of sedatives, hypnotics, anxiolytics, and anticonvulsants. As exemplified by *diazepam* (**6.5**), their

structure is characterized by a non-planar diazepine ring which inverts between *two enantiomeric boat conformations*. The conformation of the diazepine ring can be defined by four *endocyclic torsion angles* (τ_2, τ_3, τ_4, and τ_5), but it has become customary to describe the two conformers by the sign of τ_3 (the angle defined by C(2), C(3), N(4), and C(5)), namely an *(*M*)-conformer* where τ_3 is negative, and a *(*P*)-conformer* where it is positive, as shown [20–22]. These two conformers differ in the orientation of the CH_2(3) group which lies above (*M*) or below (*P*) the plane defined by the diazepine ring. Of importance is the *pseudoaxial vs. pseudoequatorial* position of the two H-atoms at C(3), to which we return in the next *Figure*. The other torsion angles are defined in the *Figure*, except the amido and imino bonds which are more rigid and near-planar.

The two enantiomeric conformers of diazepam obviously have the same conformational energy; their *ring reversal* involves a near-planar transition state of *ca*. 70 kJ/mol in which τ_3 and τ_4 assume *synperiplanar* geometries[4]). The two conformers are in very rapid equilibrium and cannot be separated physically. Nevertheless, it has been demonstrated that *serum albumin* shows a preferential affinity for the (*M*)-conformer of diazepam [23].

[4]) The ring conformations of benzodiazepines were generated during 1 ns by high-temperature MD simulations with the following characteristics: *a*) *Newton*'s equation was integrated every fs; *b*) the temperature was maintained at 1000 ± 10 K by means of *Langevin*'s algorithm; *c*) *Lennard-Jones* (*L-J*) interactions were calculated with a cut-off of 10 Å, and the pair list was updated every 20 iterations; *d*) a frame was stored every ps, yielding 1000 frames; and *f*) no constraints were applied to the systems. The obtained trajectories were analyzed to extract the (*M*)- and (*P*)-conformations which were finally minimized by a PM6 semi-empirical method.

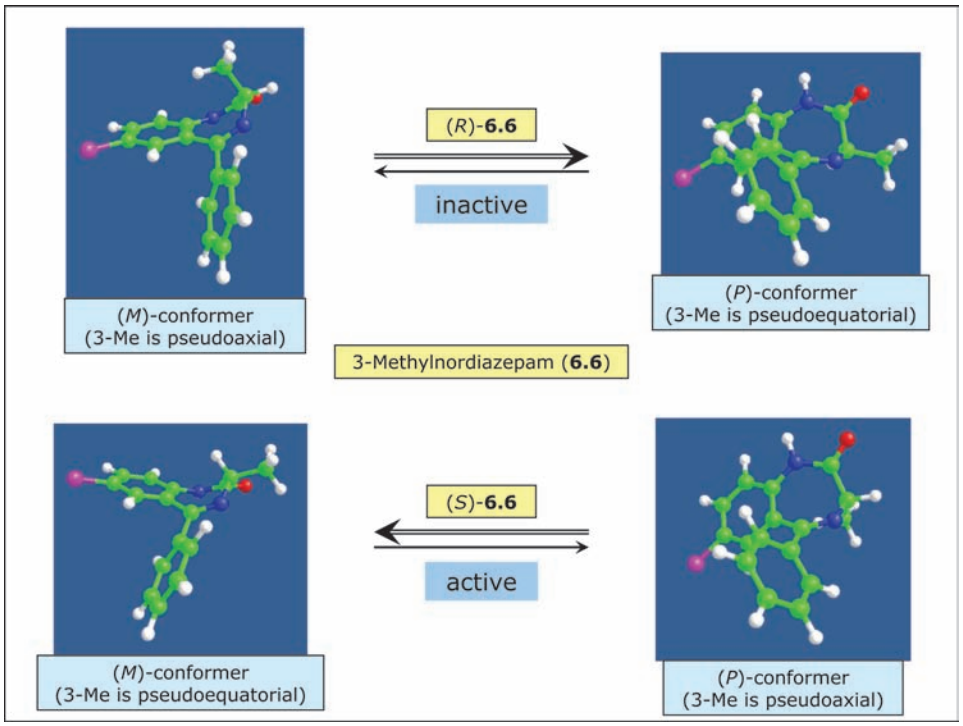

Fig. 6.9. Introdution of a small alkyl group at C(3) creates a *stable stereogenic center* giving rise to the existence of two enantiomers, as illustrated here with the model compound *3-methylnordiazepam* (**6.6**; N^1-demethyl-3-methyldiazepam) [20–22]. The creation of this stable stereogenic center results in a very high enantioselectivity in affinity to central benzodiazepine receptors. The *(*S*)-enantiomer* was consistently found to be the eutomer, with affinity ratios of *ca.* 1:1000.

As with diazepam (**6.5**), each enantiomer of 3-methylnordiazepam (**6.6**) exists predominantly as the rapidly interconverting *(*M*)- and (*P*)-conformers*, the transition state being *ca.* 50 kJ/mol. But in contrast to diazepam and analogs, the two conformers of 3-methylnordiazepam are no longer enantiomeric but *diastereoisomeric*, with the substituent at C(3) being either in a *pseudoequatorial* or a *pseudoaxial* position, as shown. The *pseudoaxial vs. pseudoequatorial* position of the 3-Me groups is a major determinant of the energy difference between the (*M*)- and (*P*)-conformers, with a pseudoequatorial position being favored by *ca.* 15 kJ/mol [20–22]. As a result and as illustrated in the *Figure*, the (*R*)-form (which is the distomer) is predominantly in the (*P*)-conformation, while the *(*S*)-eutomer prefers the (*M*)-conformation*. Based on extensive investigations with benzodiazepine receptor agonists and antagonists, several of which were *rigid molecules* (data not discussed here but extensively reviewed in [20]), it was concluded that activity is determined by the *(*M*)-conformation rather that the configuration at C(3)*.

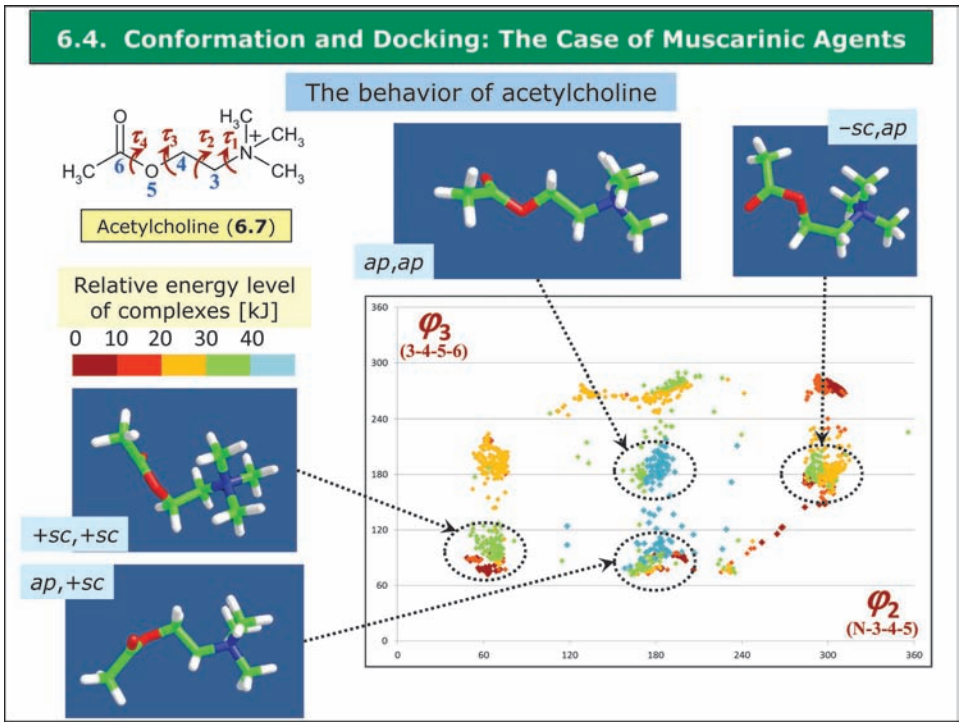

Fig. 6.10. In previous *Figures*, the conformational profiles of dopamine, methadone, and benzodiazepines were simulated *in vacuo*. Such simplified conditions seem a good starting point for conformational analyses, since the absence of solvent molecules maximizes conformational freedom even though such a low-dielectric environment favors intramolecular polar interactions. This is confirmed in the abundant literature on this topic, which also shows that polar solvents favor extended conformations.

We examine here three well-known agonists at muscarinic acetylcholine receptors, namely the neurotransmitter acetylcholine (**6.7**) and two markedly more rigid natural compounds, muscarine and pilocarpine. The three compounds were simulated under two distinct sets of conditions, *i.e.*, *in vacuo* and bound to the *human mAChR2 receptor*[5]). These molecules were chosen based on their prominent biological role, the known ability of acetylcholine (**6.7**) to adapt itself dynamically to the simulated environment, and the known 3D structure of the human mAChR2 receptor [24][25].

Acetylcholine (AcCh; **6.7**) has four dihedral angles arbitrarily defined and numbered here. Several computational studies have shown that τ_1 and τ_4 vary in a narrow range ($60 \pm 20°$ and $0 \pm 20°$, resp.) due to the symmetry of the triple rotor for τ_1 and to the rigidity of the ester group (τ_4) [24]. The structurally significant rotors in

[5]) The conformational behavior of the three selected muscarinic agonists was investigated by a clustered Monte Carlo procedure. Muscarine also underwent a 5-ns MD run *in vacuo* (*T*, 300 K; time step, 1 fs; 1000 stored frames). For each ligand, the resulting lowest-energy structure was then exploited in the subsequent docking simulations. Docking simulations on mAChR2 were performed by GriDock, a parallel tool based on the AutoDock 4.0 engine. In detail, the grid box was set to

AcCh are described by τ_2 and τ_3. Their profile (in the φ_2 and φ_3 scale) reveals a symmetrical distribution of the optimized conformers among which seven conformational clusters can easily be recognized. Among these, *three pairs of clusters* are apparent ($+sc,+sc$ and $-sc,-sc$; $+sc,ap$ and $-sc,ap$; and $ap,+sc$ and $ap,-sc$), whose relative energies are comparable pairwise, and whose angular values are mirror images. In these six clusters, stabilization appears due, in part, to favorable electrostatic interactions between the cationic head and the O-atoms. In contrast, the *fully extended (*ap,ap*) conformer* does not show these stabilizing intramolecular contacts and has a higher relative energy.

include all residues within a 15-Å radius sphere around the co-crystallized inhibitor. The resolution of the grid was $60 \times 60 \times 60$ points with a grid spacing of *ca.* 0.50 Å. For the docking simulations, the flexible bonds of the ligand were automatically recognized by GriDock and left free to rotate so as to account for ligand flexibility within the binding cavity. Each substrate was docked with the Lamarckian algorithm as implemented in AutoDock. The genetic-based algorithm ran 30 simulations per substrate with 2,000,000 energy evaluations and a maximum number of generations of 27,000. The crossover rate was increased to 0.8, and the number of individuals in each population to 150. All other parameters were left at the AutoDock default settings. The best complexes were finally minimized to favor mutual adaptability between ligand and receptor, and used to recalculate docking scores in the subsequent MD simulations. As illustrated in *Part 5*, the putative complexes were inserted in a membrane model composed of a bilayer of POPC molecules surrounded by two bands of H_2O molecules. After a preliminary minimization to optimize the relative position of membrane molecules, the systems underwent 5-ns MD runs with the following characteristics: *a*) periodic boundary conditions (PBC) were introduced to stabilize the simulation space; *b*) *Newton*'s equation was integrated by using the r-RESPA method (every 4 fs for long-range electrostatic forces, 2 fs for short-range non bonded forces, and 1 fs for bonded forces); *c*) the temperature was maintained at 300 ± 10 K by means of *Langevin*'s algorithm; *d*) *L-J* interactions were calculated with a cut-off of 10 Å, and the pair list was updated every 20 iterations; *e*) a frame was stored every 5 ps, yielding 1000 frames; *f*) no constraints were applied to the systems. The simulations were carried out in two phases: an initial period of heating from 0 to 300 K over 3000 iterations (3 ps, *i.e.*, 1 K/10 iterations) and a monitored phase of simulation of 5 ns. Only those frames memorized during this last phase were considered. All calculations were carried out by Namd2.6 using the force field CHARMM and the *Gasteiger*'s atomic charges. Further computational details can be found in [24].

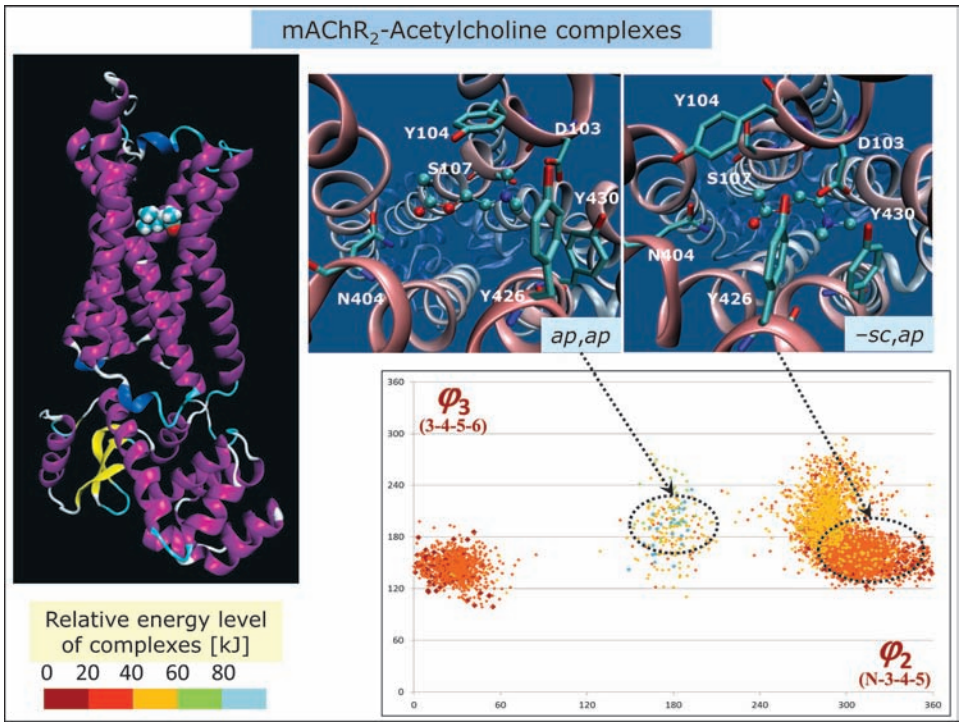

Fig. 6.11. As stated, molecular-dynamics simulations allow the formation of a complex between a ligand and its biological target to be modeled, revealing mutual adaptations and conformational constraints occurring during docking. Here, a *5-ns simulation of acetylcholine* (**6.7**) *docked into human mAChR2* was carried out. The φ_2 *vs.* φ_3 plot shows how the conformational profile of AcCh is constrained upon receptor binding.

A first observation is that AcCh is not frozen in a single conformation when bound to the mAChR2 but can assume different geometries, all of which are able to stabilize the key contacts with the receptor. This confirms that there exists not a single bioactive conformation, but that different conformers can fulfill the steric requirements necessary to optimize ligand recognition as already shown by the comparison of flexible ligands with rigid analogs. A second observation is that the torsion angles τ_2 and τ_3 do not enjoy this conformational freedom when AcCh is receptor-bound. Indeed, the plot shows that τ_2 assumes only three narrow ranges ($+sc$, *ap*, and $-sc$), whereas τ_3 can vary in the range of $-90°$ to $+120°$ ($120°$ to $270°$ in the φ scale). This can be contrasted with the behavior of AcCh *in vacuo* (*Fig. 6.10*), where we identified three pairs of approximately mirror-image clusters, plus a fully extended geometry.

When considering the relative stability of the monitored complexes as color-coded in the φ_2 *vs.* φ_3 plot, one may note that the *fully extended AcCh* shows on average poorer interaction energies compared to its complexes in which τ_2 assumes *synclinal* geometries. The explanation of this trend is clearly illustrated by the two screenshots. When assuming extended geometries, acetylcholine (**6.7**) stabilizes key interactions already apparent in other docking results, namely an ion pair between the ammonium

head and Asp103, a set of π–cation contacts with the surrounding tyrosine residues, plus a H-bond between the ester O-atoms and Asn404. When acetylcholine assumes *more folded conformations*, the ammonium head retains a similar interaction pattern, while the ester O-atom multiplies its contacts by H–bonding also with the surrounding tyrosine residues plus Ser107.

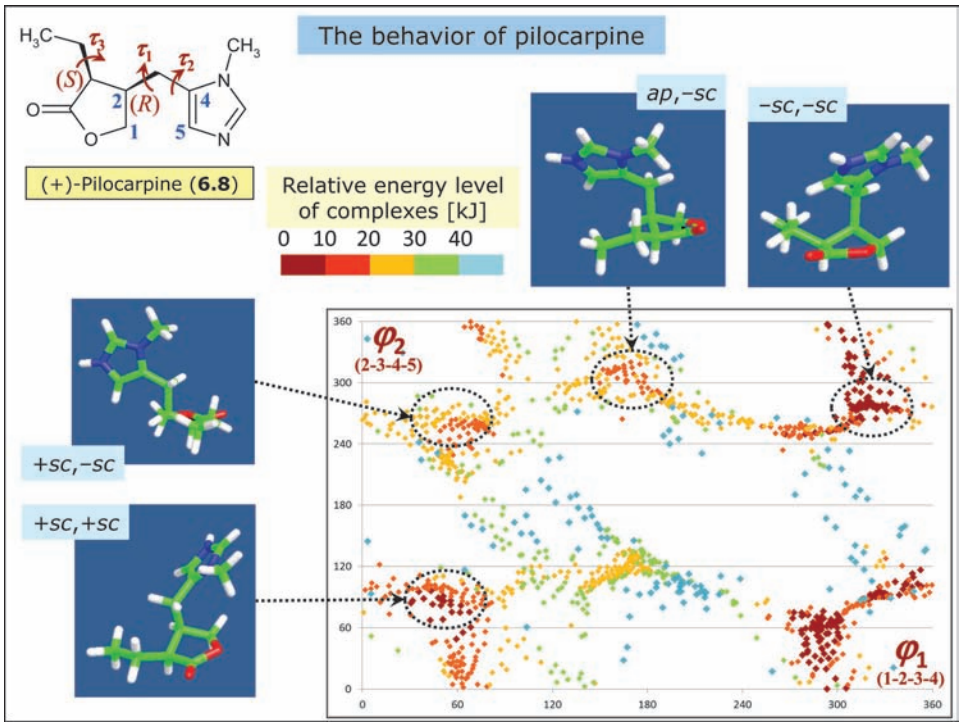

Fig. 6.12. Our second example is *pilocarpine* (**6.8**; arbitrary numbering of atoms and torsion angles), a muscarinic agonist. Here, the drug was simulated in its protonated form (pK_a *ca.* 7.0), which is the state recognized by mAChR2. Its conformational profile is essentially described by two torsion angles (τ_1 and τ_2) which modulate the reciprocal arrangement of the two rings. The third angle, τ_3, pertains to the Et chain and was ignored here due to its marginal role. The τ_1 *vs.* τ_2 plot (in the φ_1 and φ_2 scale) shows that τ_1 can assume both *synclinal* and *antiperiplanar* geometries, while τ_2 roughly assumes only *synclinal* geometries, thus yielding six conformational clusters.

When considering the energy profile of the monitored conformations, one may observe that the major factor influencing the conformational behavior of pilocarpine (**6.8**) is represented by an *intramolecular stacking* between the 1*H*-imidazole ring and the lactone ring, a contact reinforced by *protonation* of the 1*H*-imidazole ring. Such an interaction appears optimal when τ_1 and τ_2 assume a negative synclinal geometry (*i.e.*, the $-sc,-sc$ cluster), whereas, in other clusters, this contact is partly hampered by

steric hindrance between the *N*-Me and Et groups when τ_1 assumes *antiperiplanar* values. When τ_1 has positive *synclinal* values, pilocarpine (**6.8**) shows rather extended conformations, although the stacking mentioned can play a modest stabilizing role as seen in the $+sc,+sc$ conformer.

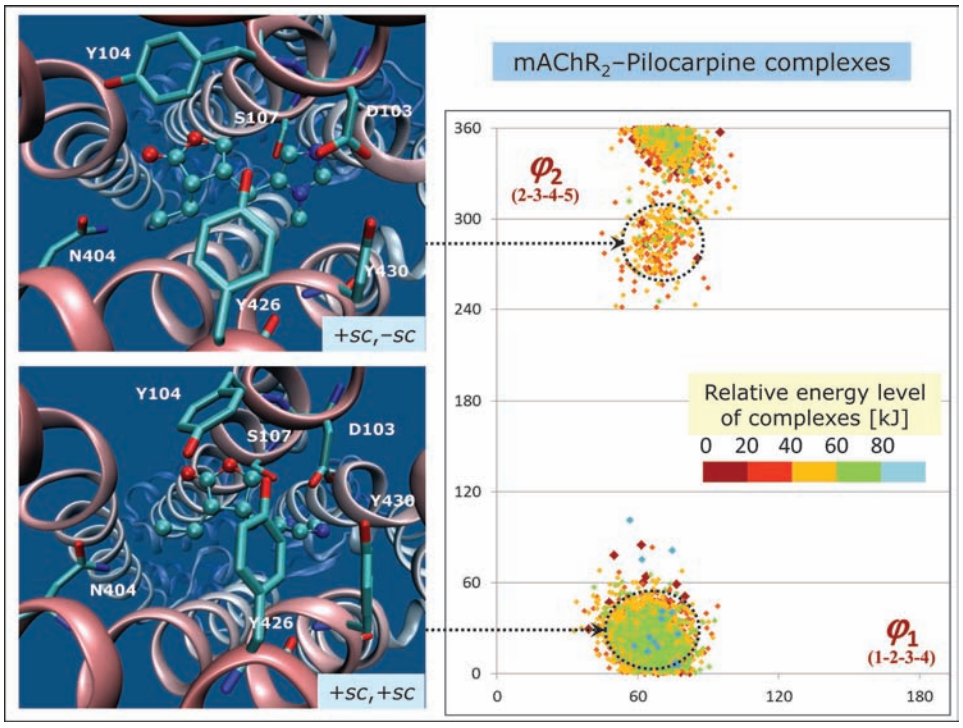

Fig. 6.13. The τ_1 *vs.* τ_2 plot (in the φ_1 and φ_2 scale) of the *pilocarpine–mAChR2 complex* shows that the conformational behavior of the ligand is heavily constrained compared to that computed *in vacuo*. Indeed, τ_1 angle is frozen in a positive *synclinal* geometry. In contrast, the τ_2 torsion angle retains more freedom, as it spans a range from $+sc$ to $-sc$, existing in two bioactive conformations with frequent interconversions passing through *synperiplanar* geometries.

Despite its rather homogeneous distribution of interaction energies, the φ_1 *vs.* φ_2 plot suggests that, on average, the more extended $+sc,-sc$ conformers of pilocarpine (**6.8**) provide more stable complexes than the $+sc,+sc$ conformers. Such a trend can be explained by the fact that only in its more *extended conformations* can pilocarpine elicit the key H-bond between its carbonyl O-atom and Asn404. Specifically, both complexes show similar interactions stabilized by the charged imidazolium ring, while some differences are seen with the lactone ring which stabilizes a richer interaction pattern when τ_2 assumes $-sc$ geometries.

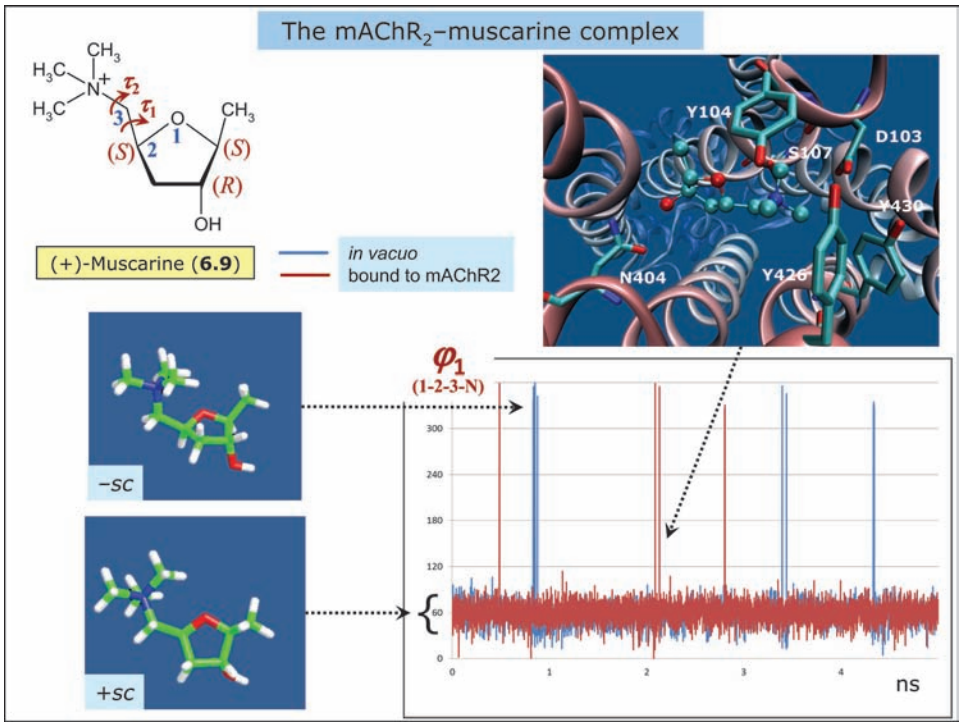

Fig. 6.14. We conclude the discussion on muscarinic ligands with natural *muscarine* (**6.9**; arbitrary numbering of atoms and torsion angles), a potent agonist found in some toxic mushrooms. The conformational profile of muscarine is defined by two rotatable bonds, even though τ_2 assumes constantly positive *synclinal* geometries due to the symmetry of the triple rotor, a conformational feature already seen with the ammonium head of acetylcholine. Hence, an investigation of the conformational profile of muscarine can be restricted to the *torsion angle* τ_1 without loss of pharmacologically significant information.

A preliminary systematic study (results not shown) revealed that τ_1 can assume only *synclinal* geometries, the $+sc$ geometries being more stable than the negative ones by *ca.* 5 kJ/mol. In particular, the conformational behavior of muscarine (**6.9**) is strongly affected by an *intramolecular H-bond between the ammonium head and the endocyclic O-atom*. This interaction is ideal when τ_1 assumes $+sc$ geometries, but is somewhat hampered for other τ_1 values by steric hindrance between the *N*-Me groups and the ring. To analyze how this modest energy difference may reflect on the relative abundance of the two possible conformers at the equilibrium, a 5-ns MD simulation was carried out *in vacuo*. The resulting plot (*blue trace*) shows that τ_1 assumes almost only $+sc$ *geometries* during the entire simulation time, while $-sc$ geometries cover less than 0.4% of the time and can be seen as rare transitions occurring during a complete rotation of the τ_1 angle. Interestingly, the same conformational behavior was observed with muscarine docked to mAChR2 (*red trace*). Also here, τ_1 assumes only $+sc$ geometries, thus suggesting that there exists *only one bioactive conformation for*

muscarine. This bioactive conformation is able to elicit all key interactions involving *a*) the ammonium head interacting with Asp103, Ser107, and the surrounding aromatic residues, and *b*) the tetrahydrofuran ring whose OH group forms a key H-bond with Asn404. One may, therefore, conclude that muscarine (**6.9**), despite its rotatable bonds, can be seen as a rigid derivative with which more flexible muscarinic ligands are to be compared to unveil the common structural features required for muscarinic agonist activity.

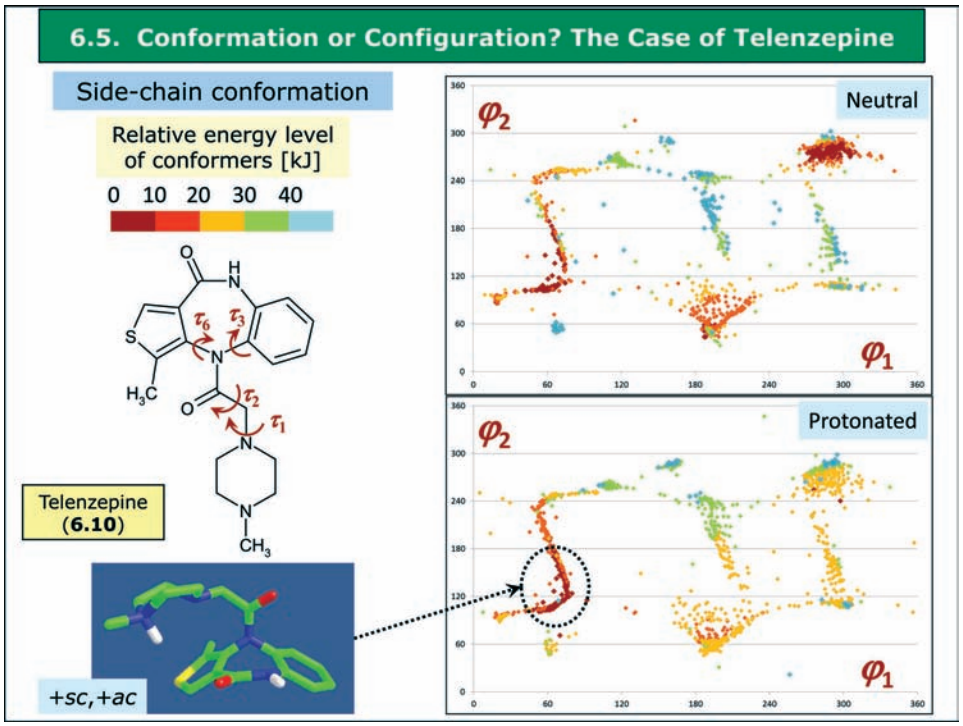

Fig. 6.15. In contrast to the four previous examples, the presentation of *telenzepine* (**6.10**; arbitrary numbering of torsion angles) does not involve an approach toward its active conformation. Indeed, our last example serves to conclude this *Part* showing some of the difficult issues raised by a complex tricyclic ring system in terms of stereochemical conventions, and conformational behavior *vs.* configurational properties.

Telenzepine (**6.10**) is an antagonist at *M1 muscarinic receptors* (mAChR1) [26]. Its chemical structure contains two main moieties, a *rather flexible side chain* whose conformational behavior will be examined first, and the *tricyclic system* mentioned above. Based on the known conformational behavior of *tricyclic drugs such as older-generation antidepressants* [27], one expects **6.10** to behave like a butterfly flapping its wings. Yet as we shall see, the two resulting geometries are not conformers but *two*

highly stable enantiomers [28]. All available pharmacological results confirm that the *(+)-enantiomer* is markedly more active than the levorotatory isomer, but the absolute configurations of the eutomer and distomer have not yet been reported.

The conformational profile of the side chain is determined mainly by two torsion angles, τ_1 and τ_2. In the *Figure*, their plots (in the φ_1 and φ_2 scale) for the neutral and protonated forms are compared. In both cases, the two angles can assume both folded and extended geometries, thus yielding nine overlapping conformational clusters whose energy profiles are influenced by two contrasting factors. There is, first, steric hindrance which tends to favor extended conformations and is particularly marked here due to the rigidity imposed by the piperazine ring and the amide bond. Second, there are attractive interactions between the piperazine N-atoms and the two aromatic rings which favor more folded geometries. These factors can also explain the observed differences between the neutral and protonated forms. Indeed, these attractive interactions are weak for the neutral side chain and at best balance the steric hindrance of the folded geometries. In contrast, the stronger charge-transfer interaction between the protonated piperazine and the aromatic rings favors folded geometries. Moreover, while the two folded clusters ($+sc, +ac$ and $-sc, -sc$) are of comparatively low energy for neutral telenzepine, the $+sc, +ac$ geometry appears to be greatly favored for the protonated form, presumably due to an additional H-bond between the ammonium head and the O-atom of the endocyclic amide moiety.

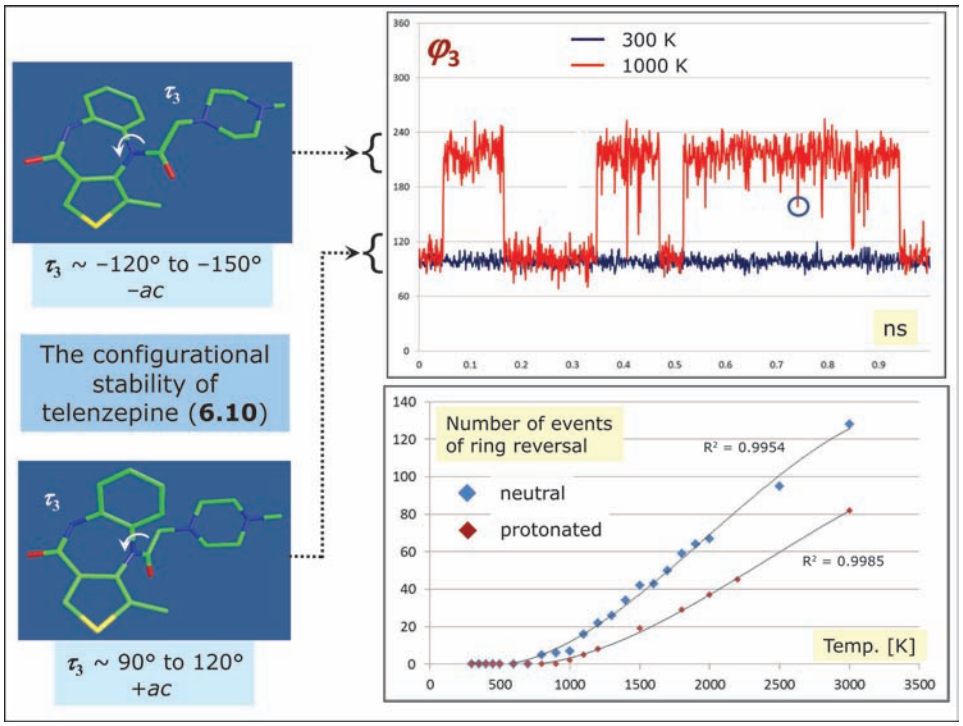

Fig. 6.16. By definition, two isomers are considered physically separable when their *half-life of interconversion* at room temperature is greater than 1,000 s (*ca.* 17 min). At room temperature and in neutral aqueous solution, the enantiomers of telenzepine (**6.10**) showed a half-life for racemization of over 1,000 years [28]. At 100°, the half-life was 48 h, and determination over a range of temperatures yielded an *energy barrier of close to 150 kJ/mol*.

Using molecular dynamics (MD) computations[6]), we have simulated the chiral ring reversal of **6.10** and monitored the number of reversal events. The starting 3D geometry was the low-energy structure with τ_3 corresponding to $+ac$ and shown in the lower left quadrant of the *Figure* (see below for the assignment of absolute configuration). The *upper plot* shows the dynamic profile of ring reversal as obtained at temperatures of 300 (*blue line*) and 1000 K (*red line*). At *300 K*, no ring reversal took place, and τ_3 fluctuated in a narrow range. At *1000 K* (an unrealistic temperature because the molecule would decompose), seven ring reversals were observed during 1 ns. This run also reveals 'failed attempts' at reversal (one of which is highlighted by a *blue circle*), namely transition states falling back to their starting structure. One also notes that τ_3 fluctuated in broader ranges compared to its fluctuation at 300 K (see also below).

[6]) Conformational analyses were carried out as described for dopamine (**6.1**). Ring reversal was investigated as described for benzodiazepines except for the temperature whose effect was monitored in the range from 300 to 3000 K.

To investigate the influence of temperature, a set of 1-ns MD runs was performed by simulating telenzepine in its neutral and protonated forms in a range of 300 – 3,000 K (*lower plot*). This range of temperature is clearly unphysical, but it offers a way to analyze the effect of increasing kinetic energy. The number of ring reversals increased almost linearly with temperature, as demonstrated by very high R^2 values, even though such events were rarer for protonated telenzepine, perhaps because the protonated form can stabilize stronger intramolecular interactions which prevent ring reversal.

Importantly, there is additional information to be obtained from these MD simulations. Indeed, our discussion up to here mentioned only the occurence of 'two enantiomers'. However, the upper plot shows quite conclusively that the torsion angle τ_3 *fluctuates inside a temperature-dependent range of values*, due to each enantiomer enjoying some *conformational freedom* in its central seven-membered ring [27]. In other words, each telenzepine enantiomer exists as *a conformational cluster* characterized by τ_3 corresponding either to $+ac$ or $-ac$. This demonstrates how the configurational and conformational properties of its ring system are intertwined. Note also that at 1,000 K the mean absolute values of τ_3 in the two enantiomeric clusters are identical, due to the broad conformational range accessible at this temperature.

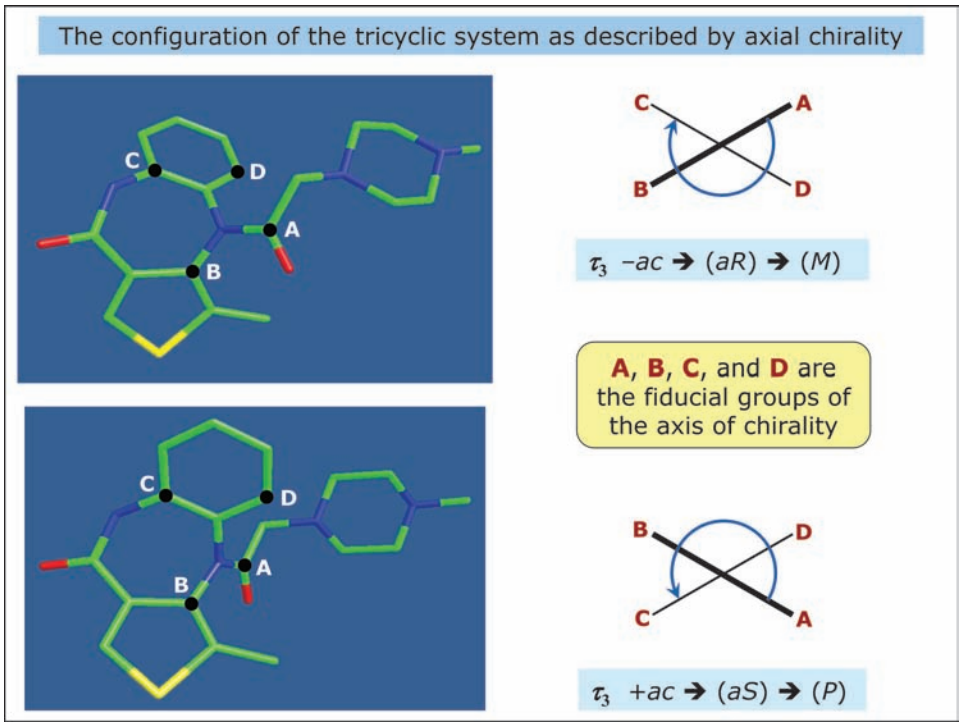

Fig. 6.17. Having documented the configurational stability and flexibility of the ring system of telenzepine (**6.10**), we must face the task of finding an adequate configurational descriptor for the two enantiomers. But as stated previously, *their respective rotation remains unknown*, so that it is currently impossible to decide which of the two enantiomers in the left-hand side of the *Figure* is the (+)-eutomer.

In an attempt to assign an unambiguous label to the two respective structures shown, *Clayden et al.* have considered telenzepine (**6.10**) to contain an *axis of chirality* (namely the N–C bond corresponding to τ_3), and they have named the two enantiomers *atropisomers* [29]. This is indeed a sensible approach given that reversal of the ring system can be described as τ_3 switching from $+ac$ *to* $-ac$ *and vice versa*. In this terminoloy, the structure with τ_3 corresponding to $-ac$ is assigned the (aR)-configuration (equivalent to (M)-helicity). In turn, the structure with τ_3 corresponding to $+ac$ has the (aS)-configuration, *i.e.*, (P)-helicity. The choice as stereogenic axis of the bond corresponding to τ_3 rather than τ_6 appears arbitrary, but choosing the latter yields the same configurational assignment.

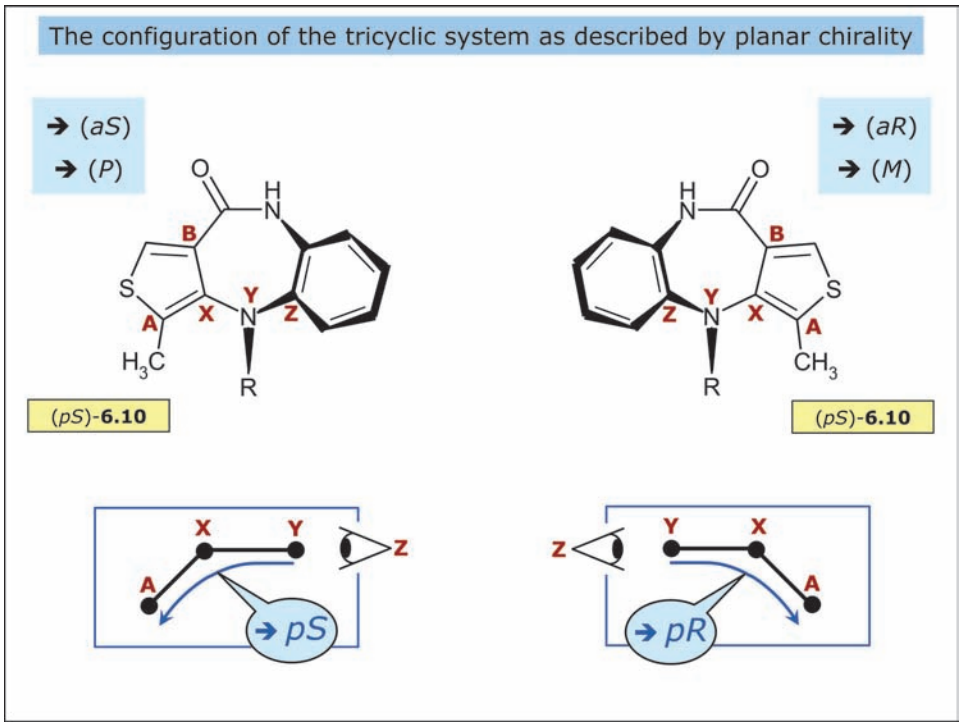

Fig. 6.18. Inspection of telenzepine (**6.10**) structure suggests an alternative approach to describe the absolute configuration of its enantiomers. Indeed, the ring system of **6.10** contains two planes, namely *a*) the benzene ring plus its two adjacent N-atoms, and *b*) the thiophene ring plus its three adjacent atoms (N, C, and C). As we saw, these two planes are not coplanar due to the butterfly structure of the ring system. The thiophene ring takes priority by virtue of the sequence rule, and it may be a *chiral plane* if other conditions are met (see *Part 3*). This is indeed the case, since viewing the chiral plane below from the *pilot atom* Z shows the atoms A–X–Y to trace a counterclockwise path in the structure of the left (*i.e.*, a (*pS*)-configuration), and a clockwise one in the structure on the right (a (*pR*)- configuration). Another example is provided by *ketotifen* in *Part 8*.

REFERENCES

[1] A. F. Casy, 'The Steric Factor in Medicinal Chemistry – Dissymmetric Probes of Pharmacological Receptors', Plenum Press, New York, 1993, 570 p.

[2] T. Carlomagno, '*NMR in Natural Products: Understanding Conformation, Configuration and Receptor Interactions*', *Nat. Prod. Rep.* **2012**, *29*, 536 – 554.

[3] C. A. Sotriffer, '*Accounting for Induced-Fit Effects in Docking: What Is Possible and What Is Not?*', *Curr. Top. Med. Chem.* **2011**, *11*, 179 – 191.

[4] J. P. Changeux, S. Edelstein, '*Conformational Selection or Induced Fit? 50 Years of Debate Resolved*', *F1000 Biol. Rep.* **2011**, *3*, 19.

[5] D. D. Boehr, R. Nussinov, P. E. Wright, '*The Role of Dynamic Conformational Ensembles in Biomolecular Recognition*', *Nat. Chem. Biol.* **2009**, *5*, 789 – 796.

[6] G. G. Hammes, Y. C. Chang, T. G. Oas, '*Conformational Selection or Induced Fit: A Flux Description of Reaction Mechanism*', *Proc. Natl. Acad. Sci. U.S.A.* **2009**, *106*, 13737 – 13741.

[7] T. R. Weikl, C. Deuster, '*Selected-Fit versus Induced-Fit Protein Binding: Kinetic Differences and Mutational Analysis*', *Proteins* **2009**, *75*, 104 – 110.

[8] T. Mavromoustakos, M. Zervou, P. Zoumpoulakis, I. Kyrikou, N. P. Benetis, L. Polevaya, P. Roumelioti, N. Giatas, A. Zoga, P. M. Minakakis, A. Kolocouris, D. Vlahakos, S. G. Grdadolnik, J. Matsoukas, '*Conformation and Bioactivity. Design and Discovery of Novel Antihypertensive Drugs*', *Curr. Top. Med. Chem.* **2004**, *4*, 385 – 401.

[9] C. Lee, '*Conformation, Action, and Mechanism of Action of Neuromuscular Blocking Muscle Relaxants*', *Pharmacol. Ther.* **2003**, *98*, 143 – 169.

[10] G. Klebe, '*Mechanisms of Stereoselective Binding to Functional Proteins*', in 'Stereochemical Aspects of Drug Action and Disposition', Eds. M. Eichelbaum, B. Testa, A. Somogyi, Springer Verlag, Berlin, 2003, pp. 183 – 198.

[11] R. Schwyzer, '*In Search of the 'Bio-Active Conformation' – Is It Induced by the Target Cell Membrane?*', *J. Mol. Recognit.* **1995**, *8*, 3 – 8.

[12] D. E. Koshland Jr., '*The Key-Lock Theory and the Induced Fit Theory*', *Angew. Chem., Int. Ed.* **1994**, *33*, 2375 – 2378.

[13] P. S. Portoghese, '*Relationships between Stereostructure and Pharmacological Activities*', *Annu. Rev. Pharmacol.* **1970**, *10*, 51 – 76.

[14] A. H. Beckett, '*The Importance of Steric, Stereochemical and Physico-Organic Features in Drug Metabolism and Drug Action*', *Pure Appl. Chem.* **1969**, *19*, 231 – 248.

[15] H. L. Komiskey, J. F. Bossart, D. D. Miller, P. N. Patil, '*Conformation of Dopamine at the Dopamine Receptor*', *Proc. Natl. Acad. Sci. U.S.A.* **1978**, *75*, 2641 – 2643; J. J. Urban, C. J. Cramer, G. R. Famini, '*A Computational Study of Solvent Effects on the Conformation of Dopamine*', *J. Am. Chem. Soc.* **1992**, *114*, 8226 – 8231.

[16] J. S. Golberg, '*Stereochemical Basis for a Unified Structure Activity Theory of Aromatic and Heterocyclic Rings in Selected Opioids and Opioid Peptides*', *Perspect. Med. Chem.* **2010**, *4*, 1 – 10.

[17] M. Froimowitz, '*Conformation-Activity Study of Methadone and Related Compounds*', *J. Med. Chem.* **1982**, *25*, 689 – 696.

[18] G. H. Loew, D. S. Berkowitz, R. C. Newth, '*Quantum Chemical Studies of Methadone*', *J. Med. Chem.* **1976**, *19*, 863 – 869.

[19] J. G. Henkel, E. P. Berg, P. S. Portoghese, '*Stereochemical Studies on Medicinal Agents. 21. Investigation of the Role of Conformational Factors in the Action of Diphenylpropylamines. Synthesis and Analgetic Potency of 5-Methylmethadone Diastereomers*', *J. Med. Chem.* **1976**, *19*, 1308 – 1314.

[20] W. Haefely, E. Kyburz, M. Gerecke, H. Möhler, '*Recent Advances in the Molecular Pharmacology of Benzodiazepine Receptors and in the Structure–Activity Relationships of Their Agonists and Antagonists*', in 'Advances in Drug Research', Vol. 14, Ed. B. Testa, Academic Press, London, 1985, pp. 165 – 322.

[21] M. Simonyi, G. Maksay, I. Kovacs, Z. Tegyey, L. Parkanyi, A. Kalman, L. Ötvös, '*Conformational Recognition by Central Benzodiazepine Receptors*', *Bioorg. Chem.* **1990**, *18*, 1 – 12.

[22] B. Paizs, M. Simonyi, '*Ring Inversion Barrier of Diazepam and Derivatives: An ab initio Study*', *Chirality* **1999**, *11*, 651 – 658.

[23] M. Pistolozzi, C. Bertucci, '*Species-Dependent Stereoselective Drug Binding to Albumin: A Circular Dichroism Study*', *Chirality* **2008**, *20*, 552 – 558.

[24] A. Pedretti, G. Vistoli, C. Marconi, B. Testa, '*Muscarinic Receptors: A Comparative Analysis of Structural Features and Binding Modes through Homology Modelling and Molecular Docking*', *Chem. Biodiversity* **2006**, *3*, 481 – 501; G. Vistoli, A. Pedretti, B. Testa, R. Matucci, '*The Conformational and Property Space of Acetylcholine Bound to Muscarinic Receptors: An Entropy Component Accounts for the Subtype Selectivity of Acetylcholine*', *Arch. Biochem. Biophys.* **2007**, *464*, 112 – 121.

[25] J. C. A. da Silva, L. C. Ducati, R. Rittner, '*Conformational and Stereoelectronic Investigations of Muscarinic Agonists of Acetylcholine by NMR and Theoretical Calculations*', *J. Mol. Struct.* **2012**, *1015*, 33 – 40.

[26] W. G. Eberlein, W. W. Engel, G. Trummlitz, G. Schmidt, R. Hammer, '*Tricyclic Compounds as Selective Antimuscarinics. 2. Structure–Activity Relationships of M1-Selective Antimuscarinics Related to Pirenzepine*', *J. Med. Chem.* **1988**, *31*, 1169 – 1174; W. G. Eberlein, W. Engel, G. Mihm, K. Rudolf, B. Wetzel, M. Entzeroth, N. Mayer, H. N. Doods, '*Structure–Activity Relationships and Pharmacological Profile of Selective Tricyclic Antimuscarinics*', *Trends Pharmacol. Sci.* **1989**, *(Dec. Suppl.)*, 50 – 54; S. W. Schmid, I. M. Modlin, L. H. Tang, A. Stoch, S. Rhee, M. H. Nathanson, G. A. Scheele, F. R. S. Gorelick, '*Telenzepine-Sensitive Muscarinic Receptors on Rat Pancreatic Acinar Cells*', *Am. J. Physiol.* **1998**, *274*, G734 – G741.

[27] M. G. Casarotto, D. J. Craik, '*Ring Flexibility within Tricyclic Antidepressant Drugs*', *J. Pharm. Sci.* **2001**, *90*, 713 – 721.

[28] C. Schudt, R. Boer, M. Eltze, R. Riedel, G. Grundler, N. J. Birdsall, '*The Affinity, Selectivity and Biological Activity of Telenzepine Enantiomers*', *Eur. J. Pharmacol.* **1989**, *165*, 87 – 96; P. Eveleigh, E. C. Hulme, C. Schudt, N. J. Birdsall, '*The Existence of Stable Enantiomers of Telenzepine and Their Stereoselective Interaction with Muscarinic Receptor Subtypes*', *Mol. Pharmacol.* **1989**, *35*, 477 – 483; U. Kilian, R. Beume, M. Eltze, D. Häfner, G. Hanauer, C. Schudt, '*Telenzepine and Its Enantiomers, M1-Selective Antimuscarinics, in Guinea Pig Lung Function Tests*', *Agents Actions Suppl.* **1991**, *34*, 131 – 147.

[29] J. Clayden, W. J. Moran, P. J. Edwards, S. R. LaPlante, '*The Challenge of Atropisomerism in Drug Discovery*', *Angew. Chem., Int. Ed.* **2009**, *48*, 6398 – 6401.

Received August 14, 2012